NASA TN D-1710



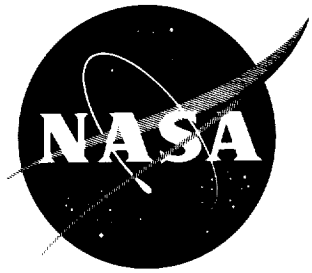


# TECHNICAL NOTE

## D-1710

# ANALYTICAL STUDY OF TURBINE-GEOMETRY CHARACTERISTICS FOR ALKALI-METAL TURBOELECTRIC SPACE POWER SYSTEMS

By Arthur J. Glassman and S. M. Futral

Lewis Research Center
Cleveland, Ohio

NATIONAL AERONAUTICS AND SPACE ADMINISTRATION
WASHINGTON

May 1963

1-3P-D

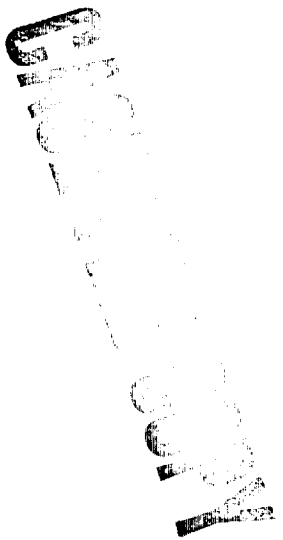

NATIONAL AERONAUTICS AND SPACE ADMINISTRATION

TECHNICAL NOTE D-1710

# ANALYTICAL STUDY OF TURBINE-GEOMETRY CHARACTERISTICS FOR ALKALI-METAL TURBOELECTRIC SPACE POWER SYSTEMS

By Arthur J. Glassman and S. M. Futral



## SUMMARY

This investigation was made primarily to determine the general effects of turbine-inlet temperature and working fluid on such turbine-geometry characteristics as number of stages, diameter, and rotative speed for a turboelectric space power system producing 1 megawatt of electric power. Sodium, potassium, rubidium, and cesium were investigated as possible working fluids with turbine-inlet temperatures ranging from 2000° to 2600° R. The molybdenum alloy containing 0.5 percent titanium and 0.07 percent zirconium (commonly referred to as TZM) was assumed for the turbine blade and disk material. The effects of varying the strength of the rotor structural material and of blade-diameter configuration on the number of stages were also considered. Possible blade-speed limitations resulting from erosion effects were recognized; because of the uncertain nature of these limitations, however, none was imposed on the results of this study.

The analysis showed that turbine-inlet temperature and working fluid exert significant effects on turbine geometry. Smaller diameter turbines that require an increasing number of stages were obtained by increasing turbine-inlet temperature. The required number of stages increased with decreasing working-fluid molecular weight. For any given temperature, turbine-stage diameters for cesium, rubidium, and potassium were nearly equal, but were considerably larger for sodium. Rotative speed, for any given number of stages, increased with temperature. Use of materials with higher ratios of strength to density and use of increasing rather than constant diameters from the first to the last stage resulted in significantly fewer stages.

## INTRODUCTION

Current NASA space-vehicle propulsion research and development programs show the need for high-power electrical systems. The interest in these systems originates from studies, such as reference 1, which show that certain advanced missions may be best achieved by the use of electrical propulsion devices. These electrical propulsion devices have an extremely high specific impulse as compared with chemical or hydrogen nuclear rockets. These studies also show that as missions become more complex and include human passengers, the power requirements for the electrical propulsion systems increase into the megawatt range.

Electric power production is one of the most critical problem areas in these systems. Presently, one of the contending methods for converting thermal energy to electric energy is the indirect power-conversion method, whereby the production of mechanical energy is an intermediate step. The indirect power-conversion system usually considered for space applications utilizes a Rankine cycle with an alkali metal as the working fluid to convert thermal energy to mechanical energy. The mechanical energy is produced by a turbine, and a generator then converts the turbine shaft power to electric power.

In considering the use of the indirect system at the high power levels desired, studies such as reference 2 have shown that extremely large radiator areas are required to reject heat from the cycle and that this area can be reduced considerably by increasing turbine-inlet temperature. Such increases, however, are limited to a great extent by allowable turbine-blade and -disk stresses.

In view of these considerations, an analytical investigation was conducted to obtain an understanding of the effect of turbine-inlet temperature and working fluid on turbine characteristics, such as number of stages, diameter, and rotative speed for a 1-megawatt power level. Sodium, potassium, rubidium, and cesium were selected as possible working fluids with turbine-inlet temperatures ranging from $2000^{\circ}$ to $2600^{\circ}$ R. The vapors were assumed to enter the turbine at their saturation temperature. Turbine-exit temperature was assumed to be three-fourths of turbine-inlet temperature, since reference 2 shows that this temperature ratio provides approximately minimum radiator area. The molybdenum alloy containing 0.5 percent titanium and 0.07 percent zirconium was selected as the material for the turbine blades and disks, since it is considered to be one of the best presently available. In addition, a comparison was made between this alloy and the molybdenum alloy containing 0.5 percent titanium only in order to show the effect of varying material strength. A turbine configuration with a linear increase in mean-section blade diameter from first to last stage was assumed for this study; however, a comparison is made with a constant mean-section blade-diameter configuration in order to show the effects of this variation.

## SYMBOLS

| | |
|---|---|
| $A$ | area, sq ft |
| $\mathscr{A}$ | aspect ratio, $l/t_{b,r}$ (see fig. 1) |
| $d$ | mean-section blade diameter, ft |
| $e$ | disk taper parameter, $t_{d,c}/t_{d,r}$ (see fig. 1) |
| $g$ | acceleration due to gravity, 32.17 ft/sec$^2$ |
| $\Delta h$ | specific work or specific enthalpy, Btu/lb |
| $J$ | mechanical equivalent of heat, 778.2 ft-lb/Btu |
| $l$ | blade height, ft |
| $M$ | Mach number |

| | |
|---|---|
| $m$ | moisture, weight fraction |
| $N$ | rotative speed, rpm |
| $n$ | number of turbine stages |
| $P$ | power, kw |
| $Re$ | Reynolds number, as defined in ref. 3 |
| $r$ | radius, ft |
| $s$ | stress, psf |
| $s_a$ | allowable stress, psf |
| $st$ | stage number |
| $T$ | temperature, $^{o}R$ |
| $t_{b,r}$ | axial blade chord and rim thickness, ft |
| $t_{d,c}$ | disk thickness at centerline, ft |
| $t_{d,r}$ | disk thickness at rim, ft |
| $U$ | mean-section blade speed, ft/sec |
| $U_{eff}$ | effective mean-section blade speed used to define overall performance parameters, ft/sec |
| $V$ | absolute gas velocity, ft/sec |
| $W$ | relative gas velocity, ft/sec |
| $w$ | turbine weight flow, lb/sec |
| $\alpha$ | mean-section stator exit angle measured from axial direction, deg |
| $\eta$ | efficiency |
| $\lambda$ | speed-work parameter, $U^2/gJ\ \Delta h_{aer}$ |
| $\overline{\nu}$ | overall blade- to jet-speed ratio, $U/\sqrt{2gJ\ \overline{\Delta h}_{id}}$ |
| $\rho$ | vapor density, lb/cu ft |
| $\rho_m$ | density of disk and blade material, 637 lb/cu ft |
| $\omega$ | angular velocity, radians/sec |

Subscripts:

| | |
|---|---|
| aer | aerodynamic |
| an | annulus |
| b | blade |
| d | disk |
| e | station at turbine exit |
| G | generator |
| h | hub |
| i | station at turbine inlet |
| id | ideal |
| n | last stage |
| re | station at rotor exit |
| s | static conditions |
| se | station at stator exit |
| st | stage number, st = 1, 2, . . ., n |
| T | vapor turbine |
| t | tip |
| u | tangential component |
| x | axial component |

Superscript:

| | |
|---|---|
| — | overall |

## METHOD OF ANALYSIS

The basic approach to the analysis, along with the simplifying assumptions, will be discussed before the details of the calculation procedure are presented.

### Design Criteria

Since this is a parameteric analysis that is being made for the purpose of

determining the general effects of such factors as turbine-inlet temperature and fluid on turbine geometry and not a design analysis for a specific application, certain simplifying assumptions are made concerning turbine configuration. These assumptions are

(1) Stator-exit angle is equal to $70^{\circ}$.

(2) Ratio of rotor- to stator-exit axial kinetic energy is equal to 1.5.

(3) Stage speed-work parameter is constant for a given turbine and equal to the product of overall speed-work parameter and number of stages ($\lambda_{st} = n\bar{\lambda}$).

(4) Blade diameter increases linearly from first to last stage except where noted.

(5) Blade aspect ratio and disk taper parameter are equal to 2 and 2.5, respectively, (see fig. 1).

(6) Last stage is designed for equal stress in blade hub and disk.

All angles, velocities, and diameters except where otherwise noted refer to those at the blade mean section.

Performance. - Generalized turbine performance characteristics are presented in reference 3 for multistage gas turbines with constant blade diameters. Overall aerodynamic efficiency is correlated with overall blade- to jet-speed ratio, which is defined as

$$\bar{\nu} = \frac{U}{\sqrt{2gJ\ \overline{\Delta h}_{id}}}$$

and overall speed-work parameter, which is defined as

$$\bar{\lambda} = \frac{U^2}{gJ\ \overline{\Delta h}_{aer}}$$

In this study, the working fluid is not a gas, but a condensing vapor; and the turbine does not have a constant blade diameter, but one that increases linearly from first to last stage. Consequently, in order to apply the results of reference 3 to this study, the aforementioned performance parameters must be either related to or redefined in terms of this study.

In this case of a condensing-vapor turbine, not only must aerodynamic losses be considered, but also those losses resulting from either (1) the impact of the liquid droplets on the rotating blades or (2) a reduction in available energy due to the occurrence of supersaturation. An efficiency loss of 0.10 is assumed to cover the moisture and supersaturation effects; therefore, the required aerodynamic efficiency must exceed the overall turbine efficiency by 0.10.

The previously mentioned performance parameters $\bar{\nu}$ and $\bar{\lambda}$ are both defined in terms of a constant blade speed. For the purposes of this investigation, $\bar{\nu}$ and $\bar{\lambda}$ are redefined in terms of an effective blade speed as

$$\bar{\lambda} = \frac{U_{eff}^2}{gJ\ \overline{\Delta h}_{aer}}$$

and

$$\bar{\nu} = \frac{U_{eff}}{\sqrt{2gJ\ \overline{\Delta h}_{id}}}$$

The appropriate value of effective blade speed can be determined by expressing stage work in terms of stage speed-work parameter and applying assumption (3):

$$\Delta h_{st,aer} = \frac{U^2}{gJ\lambda_{st}} = \frac{U^2}{gJn\bar{\lambda}}$$

Summing turbine work over all stages gives

$$\overline{\Delta h}_{aer} = \sum_{st=1}^{n} \Delta h_{st,aer} = \frac{1}{gJn\bar{\lambda}} \sum_{st=1}^{n} U^2$$

and then solving for $\bar{\lambda}$ yields

$$\bar{\lambda} = \frac{\frac{1}{n} \sum_{st=1}^{n} U^2}{gJ\ \overline{\Delta h}_{aer}}$$

Comparing this expression with the redefined $\bar{\lambda}$ shows that

$$U_{eff}^2 = \frac{1}{n} \sum_{st=1}^{n} U^2$$

Consequently, the effective blade speed to be used in the definition of the turbine performance parameters is the root-mean-square speed.

Stress. - In this analysis, stress limitations are considered in the first and last stages. The assumption of increasing blade diameter from first to last stage was made in order to utilize the higher allowable stresses as the tempera-

ature is reduced. Within the limitations of this analysis, however, the procedure did not, in general, result in a configuration where both the first and the last stages are stressed to their allowable limits. If the last stage is assumed to operate at its allowable stress limit, then, within the framework of the assumptions, many cases are found where the solution yields turbines with first stages too small to pass the required flow. If the first-stage disk is assumed to operate at its stress limit, however, a satisfactory solution results for all cases. Consequently, the stress criterion for the selected turbine designs is a limiting stress in the first-stage disk.

The material selected for this study was the molybdenum-base alloy containing 0.5 percent titanium and 0.07 percent zirconium. This alloy is commonly known as TZM and was selected on the basis of its favorable strength-temperature characteristics. Blade and disk allowable stresses were set at those resulting in 1 percent creep in 10,000 hours. This allowable stress was estimated by using 50 percent of the 10,000-hour rupture stress extrapolated from the data of reference 4 and can be expressed as

$$s_a = 2.261\times10^{8} \exp(-1.82\times10^{-3}\ T) \qquad (\text{lb/sq ft})$$

The blade or disk temperature that will be used in this equation is the static temperature of the vapor at the specified location. Since vapor-liquid phase equilibrium is assumed in the turbine, it is postulated that the enthalpy rise due to fluid impingement on the blades will cause no rise in temperature but only vaporization of some of the condensate.

## Procedure

Generator power output is related to fluid enthalpy drop in the turbine by

$$P_G = 1.054\ \eta_G \overline{\eta}_T w\ \overline{\Delta h}_{id} \qquad (\text{kw})$$

When it is assumed that $\eta_T = 0.70$, $\eta_G = 0.85$, and $P_G = 1000$, an expression is obtained for turbine weight flow:

$$w = \frac{1595.3}{\overline{\Delta h}_{id}} \qquad (\text{lb/sec}) \qquad (1)$$

Overall performance. - Figure 2, obtained by the procedure presented in reference 3, presents a set of generalized multistage turbine performance characteristics relating overall aerodynamic static efficiency $\overline{\eta}_{s,aer}$ to number of stages $n$ and blade- to jet-speed ratio $\overline{\nu}$. At this point in the calculation a value for $n$ is assumed, and the value of $\overline{\nu}$ required to yield the necessary $\overline{\eta}_{s,aer} = 0.80$ is obtained from figure 2. The effective blade speed is then determined from the equation defining $\overline{\nu}$:

$$U_{eff} = \overline{\nu}\ \sqrt{2gJ\ \overline{\Delta h}_{id}} \qquad (\text{ft/sec}) \qquad (2)$$

The fluid properties were obtained from reference 5 and are shown in figure 3; $\overline{\Delta h}_{id}$ is given in figure 3(a). The overall speed-work parameter $\bar{\lambda}$ is then computed from its definition:

$$\bar{\lambda} = \frac{U_{eff}^2}{gJ\,\overline{\Delta h}_{aer}} \tag{3}$$

where

$$\overline{\Delta h}_{aer} = \bar{\eta}_{aer}\,\overline{\Delta h}_{id} \qquad \text{(Btu/lb)} \tag{4}$$

The stage speed-work parameter, according to assumption (3), is

$$\lambda_{st} = n\bar{\lambda} \tag{5}$$

The criterion for turbine selection, as mentioned previously, is a limiting stress in the first-stage disk. It appears, however, that there is no direct manner in which to apply this criterion and obtain a solution. The last-stage characteristics must be computed first, followed by the first-stage characteristics. Only after the last- and first-stage characteristics are known, can it be determined whether the analysis criterion is satisfied.

Last stage. - The blade speed can be related to the blade stress in the last stage. An equation for blade stress is derived in reference 6 as

$$s_b = \frac{\rho_m \omega^2 r_t^2}{2g}\left[1 - \left(\frac{r_h}{r_t}\right)^2\right] \qquad \text{(lb/sq ft)}$$

Expressed in terms of blade speed, the angular velocity is

$$\omega = \frac{2U}{r_h + r_t} \qquad \text{(rad/sec)}$$

and rearrangement of the expression for blade stress yields

$$U = \sqrt{\frac{gs_b}{2\rho_m}\,\frac{1 + \frac{r_h}{r_t}}{1 - \frac{r_h}{r_t}}} \qquad \text{(ft/sec)} \tag{6}$$

Last-stage hub- to tip-radius ratio can be determined from the analysis assumptions and the following equation (ref. 6), which relates both the blade and

the disk stresses to rotor geometric features:

$$e = \exp\left[\frac{\rho_{m,d} s_b}{\rho_{m,b} s_d} \frac{\left(\frac{1 + \frac{r_h}{r_t}}{1 - \frac{r_h}{r_t}} - 1 - \frac{2}{\mathscr{A}}\right)^2}{4\left(\frac{1 + \frac{r_h}{r_t}}{1 - \frac{r_h}{r_t}}\right)}\right] \tag{7}$$

Figure 1 shows a typical turbine rotor and indicates the parameters used in equation (7). In this equation, $\mathscr{A} = 2$ and $e = 2.5$, as specified in assumption (5), $s_b = s_d$, as specified in assumption (6), and $\rho_{m,b} = \rho_{m,d}$, because the same material is assumed for both blades and disk. After substitution of the assumed values, solution of equation (7) yields a last-stage hub- to tip-radius ratio approximately equal to 0.75. Using this value of $r_h/r_t$ in equation (6) results in the desired equation:

$$U_n = \sqrt{\frac{7 g s_{b,n}}{2\rho_m}} \quad \text{(ft/sec)} \tag{8}$$

As a first assumption, the last-stage blade stress is set equal to its maximum allowable value which, as mentioned previously, can be expressed as

$$s_a = 2.261 \times 10^8 \exp(-1.82 \times 10^{-3}\, T) \quad \text{(lb/sq ft)} \tag{9}$$

where, for the last stage, the turbine-exit temperature is used for $T$.

The last-stage velocity characteristics can now be determined. Figure 4 shows a typical stage velocity diagram, which can be used to help follow the discussion. The change in tangential velocity across a stage can be expressed as

$$\Delta V_{u,st} = \frac{U}{\lambda_{st}} \quad \text{(ft/sec)} \tag{10}$$

The relations between the rotor-inlet and -exit tangential velocities and the stage speed-work parameter are given in reference 3:

For $0 \leq \lambda_{st} \leq 0.5$:

$$V_{u,se} = \left(\lambda_{st} + \frac{1}{2}\right) \Delta V_{u,st} \quad \text{(ft/sec)} \tag{11a}$$

$$V_{u,re} = \left(\lambda_{st} - \frac{1}{2}\right) \Delta V_{u,st} \quad \text{(ft/sec)} \tag{11b}$$

For $0.5 \leq \lambda_{st} \leq 1.0$:

$$V_{u,se} = \Delta V_{u,st} \qquad \text{(ft/sec)} \tag{11c}$$

$$V_{u,re} = 0 \tag{11d}$$

With the value of $\Delta V_{u,n}$ determined from $U_n$ and equation (10), the last-stage rotor-inlet and -exit tangential velocities are calculated from equations (11).

The axial velocity at the stator exit is obtained from

$$V_{x,se} = V_{u,se} \cot \alpha \qquad \text{(ft/sec)} \tag{12a}$$

where $\alpha$ is assumed to be $70^{\circ}$, as specified in assumption (1). According to assumption (2), the ratio of rotor- to stator-exit axial kinetic energy is equal to 1.5. Consequently,

$$V_{x,re} = V_{x,se} \sqrt{1.5} \qquad \text{(ft/sec)} \tag{12b}$$

Last-stage blade diameter is determined from the annulus area necessary to pass the required weight flow and the specified hub- to tip-radius ratio. Annulus area can be computed from

$$A_{an} = \pi d^2 \frac{\left(1 - \frac{r_h}{r_t}\right)}{\left(1 + \frac{r_h}{r_t}\right)} \qquad \text{(sq ft)} \tag{13a}$$

Using the last-stage hub- to tip-radius ratio of 0.75 and rearranging equation (13a) yield

$$d_n = \sqrt{\frac{7}{\pi} A_{an,n}} \qquad \text{(ft)} \tag{13b}$$

The last-stage annulus area at the rotor exit is calculated from the continuity equation as

$$A_{an,n,re} = \frac{w(1 - m_e)}{\rho_{n,re} V_{x,re,n}} \qquad \text{(sq ft)} \tag{14}$$

where $m$ and $\rho$ were obtained from reference 5 and are shown in figure 3(b) and (c), respectively. Phase equilibrium is assumed at the rotor exit, and the volume occupied by the condensed liquid is neglected because of the much greater volume of the remaining vapor. The annulus area computed from equation (14) is used to compute the last-stage blade diameter from equation (13b). Turbine rotative speed is then obtained from

$$N = \frac{60U_n}{\pi d_n} \qquad \text{(rpm)} \tag{15}$$

The last-stage characteristics are thus determined, and consideration is now given to the first stage.

First stage. - The first-stage blade speed can be computed from the effective and the last-stage blade speeds and assumption (4), which specifies a linear increase in blade diameter, and consequently in blade speed, with stage number. The linear increase in speed with stage number can be expressed as

$$U = \frac{U_n - U_1}{n - 1}(st - 1) + U_1 \qquad \text{(ft/sec)} \tag{16}$$

where $U$ is the blade speed of the $(st)^{th}$ stage. The effective blade speed is

$$U_{eff} = \sqrt{\frac{1}{n}\sum_{st=1}^{n} U^2} \qquad \text{(ft/sec)} \tag{17}$$

Substituting equation (16) into equation (17) and performing the summation yield

$$(2n - 1)U_1^2 + 2(n - 2)U_nU_1 + (2n - 1)U_n^2 - 6(n - 1)U_{eff}^2 = 0 \tag{18}$$

Equation (18) is a quadratic equation that can be solved for $U_1$. Examination of equation (18) shows that for $n > 1$ there can be no more than one positive root for $U_1$; however, there may be no positive roots, but two negative or two imaginary roots. If a positive root is obtained, the calculation procedure is continued with this root. If both roots are negative or imaginary, either the assumed number of stages or the assumed last-stage blade stress is too high, and new assumptions for one or the other of these values must be made and the calculation repeated until a positive $U_1$ is obtained.

With $U_1$ known, the first-stage blade diameter is computed by

$$d_1 = \frac{60U_1}{\pi N} \qquad \text{(ft)} \tag{19}$$

The first-stage velocity characteristics are calculated from equations (10) to (12). Annulus area at the first-stage stator exit is obtained from the continuity equation as

$$A_{an,1,se} = \frac{w(1 - m_{1,se})}{\rho_{1,se}V_{x,se,1}} \qquad \text{(sq ft)} \tag{20}$$

Phase equilibrium is assumed, and the volume occupied by the condensed liquid is

neglected because of the much greater volume of the vapor. The temperature at the stator exit must be determined in order to obtain the moisture and density terms in equation (20).

The enthalpy drop across the first-stage stator can be determined from

$$\Delta h_1 = \frac{V_{se,1}^2}{2gJ} = \frac{V_{u,se,1}^2 + V_{x,se,1}^2}{2gJ} \qquad \text{(Btu/lb)} \tag{21}$$

if a nozzle coefficient of 1.0 is assumed. With the enthalpy drop computed from equation (21), the temperature and moisture content of the fluid can be obtained from the data of reference 5, and the annulus area evaluated by equation (20). The first-stage hub- to tip-radius ratio is then computed by rearranging equation (13):

$$\frac{r_h}{r_t} = \frac{1 - \frac{A_{an}}{\pi d^2}}{1 + \frac{A_{an}}{\pi d^2}} \tag{22}$$

The first-stage blade stress can now be computed by rearranging equation (6):

$$s_b = \frac{2\rho_m U^2}{g}\left(\frac{1 - \frac{r_h}{r_t}}{1 + \frac{r_h}{r_t}}\right) \qquad \text{(lb/sq ft)} \tag{23}$$

and the disk stress is computed by rearranging equation (7) and substituting the specified parameter values:

$$s_d = \frac{s_b}{\ln 2.5} \frac{\left(\frac{1 + \frac{r_h}{r_t}}{1 - \frac{r_h}{r_t}} - 2\right)^2}{4\left(\frac{1 + \frac{r_h}{r_t}}{1 - \frac{r_h}{r_t}}\right)} \qquad \text{(lb/sq ft)} \tag{24}$$

The allowable stress for the first stage is computed from equation (9) by using the previously determined stator-exit temperature. For any set of input conditions, the desired solution is the turbine with the least number of stages operating with the first-stage disk at its maximum allowable stress and the first-stage blades and last-stage disk and blades at or below their maximum allowable stresses. Iteration with respect to both number of stages and last-stage stress

is required in order to obtain the specified solution.

## RESULTS OF ANALYSIS

The results of this analysis were obtained by using only an integral number of stages for the computations. Consequently, smooth curves were not obtained, and the results are plotted as discrete calculated points with interconnecting straight lines for ease in following the trends. It was recognized that blade-speed limitations may be necessary in order to minimize erosion damage to the blades. Since the nature of these limitations for the blading materials and working fluids used in this study is completely unknown, none was imposed on the results of the analysis.

### Effect of Turbine-Inlet Temperature and Fluid

The effects of turbine-inlet temperature and fluid on number of stages, turbine stage diameters, blade speed, and rotative speed were determined with a ratio of turbine-exit to -inlet temperature of 0.75 assumed. Preliminary computations showed that a variation in turbine temperature ratio between 0.6 and 0.8 had, in general, little effect on turbine geometry.

Number of stages. - The required number of turbine stages as a function of turbine-inlet temperature is presented in figure 5 for the four fluids. As the turbine-inlet temperature increases from 2000° to 2600° R, the number of stages required with cesium remains constant at one, while the number of stages required with rubidium, potassium, and sodium increases from one to two, two to three, and three to six, respectively. The intermediate temperatures at which the step increases in number of stages are shown were determined in a manner to be described during the discussion of last-stage blade speed (fig. 6).

The increase in required number of stages with increasing turbine-inlet temperature is due to the decreasing strength of the rotor structural material. As allowable stress decreases, blade speed must also decrease; consequently, the work per stage is reduced, and more stages are required to do a specified amount of work. The variation in number of stages with working fluid results from the variation in fluid specific work. For given turbine-inlet and -exit temperatures, specific work is approximately inversely proportional to molecular weight (see fig. 3(a)). (The molecular weights for sodium, potassium, rubidium, and cesium are 23.0, 39.1, 85.5, and 132.9, respectively.) Increasing specific work reduces blade- to jet-speed ratio and, as can be seen from figure 2, results in an increase in number of stages in order to maintain a given efficiency.

Blade speed. - For the turbines considered in this analysis, the highest blade speed is encountered in the last stage, where the diameter is largest. In order to show the blade speeds that may be encountered in the design of alkali-metal turbines, the last-stage blade speed is presented in figure 6 as a function of turbine-inlet temperature for the four fluids. Also shown in this figure is the curve representing the maximum allowable blade speed, as determined from equations (8) and (9). As the turbine-inlet temperature increases from 2000°

to 2600° R, the maximum allowable last-stage blade speed decreases from 1615 to 1070 feet per second. This decrease in blade speed, as mentioned previously, is due to the decrease in material strength.

The sharp breaks in each curve correspond to an increase in the required number of stages, as can be seen in figure 5. The temperature at which a given step change occurs was estimated by extending the portion of a curve representing blade speed for a constant number of stages to intersect the maximum-allowable-blade-speed curve. This temperature was then used in figure 5 to locate the step increase in number of stages.

Turbine diameter. - The last-stage blade diameter is presented in figure 7 as a function of turbine-inlet temperature for the four fluids. As the turbine-inlet temperature increases from 2000° to 2600° R, the last-stage blade diameter decreases from 21.4 to 7.8 inches, 22.2 to 8.1 inches, 23.0 to 7.3 inches, and 45.5 to 11.5 inches with rubidium, cesium, potassium, and sodium, respectively. Since the last-stage hub- to tip-radius ratio is assumed constant, the last-stage diameter is solely a function of the annulus area required to pass the system weight flow. Consequently, the effects of temperature and fluid on last-stage diameter depend only on continuity considerations (eq. (14)). As the temperature increases, the primary effect is an increase in fluid density which results in a decreasing annulus area. The very low vapor density of sodium results in large diameters for sodium turbines. For the other three fluids, the various terms of the continuity equation offset each other to yield nearly equal last-stage diameters at any given temperature. For the multistage turbines, the ratios of last- to first-stage blade diameter are nearly constant for each fluid over the investigated temperature range (1.2, 1.5, and 1.75 for rubidium, potassium, and sodium, respectively).

Rotative speed. - Turbine rotative speed as a function of turbine-inlet temperature is presented in figure 8 for the four fluids. As the turbine-inlet temperature increases from 2000° to 2600° R, the rotative speed increases from a range of 7600 to 13,500 to a range of 19,600 to 31,400 rpm. Rotative speed is directly proportional to blade speed and inversely proportional to blade diameter (eq. (15)). Although blade speed decreases, the relatively large decrease in diameter with increasing temperature causes an increase in rotative speed.

## Effect of Structural Material and Blade Diameter Configuration

The results presented thus far were obtained with TZM as the structural material for a rotor, the blade diameter of which increased linearly from the first to the last stage. The effects of structural material and turbine shape on the number of stages are shown in figure 9, where the number of turbine stages for a potassium turbine is plotted against turbine-inlet temperature for three cases: (1) a TZM rotor with a blade diameter that increases linearly from the first to the last stage, (2) a rotor made from the molybdenum alloy containing 0.5 percent titanium (Mo-0.5Ti) with a blade diameter that increases linearly from the first to the last stage, and (3) a Mo-0.5Ti rotor with a constant blade diameter. This figure shows that, for the temperature range of 2000° to 2600° R, a significant reduction in the required number of stages (from 20 to 40 percent) can be

achieved by allowing blade diameter to increase linearly from the first to the last stage instead of remaining constant. It also shows that a further significant reduction in number of stages (from 25 to 50 percent) can be achieved by using TZM, which has a ratio of strength to density about twice that of Mo-0.5Ti, instead of Mo-0.5Ti as the rotor structural material. Both of these effects result from the utilization of higher allowable blade speeds in order to yield more work per stage.

## Turbine Characteristics for Inlet Temperature of 2500° R

Since the radiator is by far the heaviest component in a turboelectric space power system, overall system weight is significantly reduced by a reduction in radiator weight. As pointed out in reference 2, radiator area is significantly reduced by an increase in turbine-inlet temperature. With a turbine-inlet temperature of 2500° R, for example, the radiator area is about one-third that required with a turbine-inlet temperature of 1900° R. Consequently, it is desirable to operate turboelectric space power systems with as high a turbine-inlet temperature as practical. For the near future, it is believed that a turbine-inlet temperature of 2500° R can be achieved. The pertinent geometric characteristics for turbines using cesium, rubidium, potassium, and sodium and operating with an inlet temperature of 2500° R and an exit- to inlet-temperature ratio of 0.75 are presented schematically in figure 10 and are tabulated as follows:

| Characteristic | Fluid | | | |
|---|---|---|---|---|
| | Sodium | Potassium | Rubidium | Cesium |
| Number of stages | Five | Three | Two | One |
| Diameter, in. | | | | |
| First stage | 7.16 | 5.64 | 7.68 | ---- |
| Last stage | 13.28 | 8.68 | 9.00 | 9.15 |
| Rotative speed, rpm | 19,556 | 26,758 | 19,323 | 23,545 |

The last-stage velocity diagrams for these four turbines are presented in figure 11. For the multistage turbines, the velocity diagrams for the other stages are geometrically similar to that for the last stage. The last-stage stator-exit velocities are supersonic for all four turbines. Mach numbers were computed from sonic velocities obtained from the considerations of reference 7. The sodium turbine operates with impulse rotor conditions and a very small amount of negative exit whirl, while the potassium, the rubidium, and the cesium turbines operate with positive rotor reaction and zero exit whirl.

## SUMMARY OF RESULTS

This investigation was undertaken primarily to determine the effects of turbine-inlet temperature and working fluid on such turbine characteristics as

number of stages, diameter, and rotative speed for a turboelectric space power system producing 1 megawatt of electric power. The molybdenum alloy containing 0.5 percent titanium and 0.07 percent zirconium (commonly referred to as TZM) was assumed for the turbine blade and disk material. Possible blade-speed limitations resulting from erosion effects were recognized; because of the uncertain nature of these limitations, however, none was imposed on the results of this study. The following pertinent results were obtained from this analysis:

1. An increase in turbine-inlet temperature from 2000° to 2600° R resulted in (a) an increase in the required number of stages due to a reduction in allowable stress and (b) a decrease in blade diameters due to an increase in vapor density. Rotative speed increased with temperature because of the relatively large decrease in diameter.

2. Decreasing the working-fluid molecular weight (which corresponds to going from cesium to rubidium to potassium to sodium) resulted in an increase in the required number of stages because the specific work increased. For any given temperature, the blade diameters were nearly equal for cesium, rubidium, and potassium but were considerably larger for sodium because of its low vapor density.

3. Significant reductions in the required number of stages were obtained by both (a) using a rotor structural material with an increased ratio of strength to density and (b) employing a configuration with a blade diameter that increases from the first to the last stage rather than a constant blade diameter.

4. At a turbine-inlet temperature of 2500° R, a goal believed to be achievable in the near future, and a ratio of turbine-exit to -inlet temperature of 0.75, the pertinent turbine geometry characteristics are as follows:

| Characteristic | Fluid | | | |
|---|---|---|---|---|
| | Sodium | Potassium | Rubidium | Cesium |
| Number of stages | Five | Three | Two | One |
| Diameter, in. | | | | |
| First stage | 7.16 | 5.64 | 7.68 | ---- |
| Last stage | 13.28 | 8.68 | 9.00 | 9.15 |
| Rotative speed, rpm | 19,556 | 26,758 | 19,323 | 23,545 |

Lewis Research Center
National Aeronautics and Space Administration
Cleveland, Ohio, February 6, 1963

## REFERENCES


1. Koerner, Terry W., and Paulson, John J.: Nuclear Electric Power for Space Missions. TR 34-230, Jet Prop. Lab., C.I.T., 1961.

2. Moffitt, Thomas P., and Klag, Frederick W.: Analytical Investigation of Cycle Characteristics for Advanced Turboelectric Space Power Systems. NASA TN D-472, 1960.

3. Stewart, Warner L.: A Study of Axial-Flow Turbine Efficiency Characteristics in Terms of Velocity Diagram Parameters. Paper 61-WA-37, ASME, 1961.

4. Houck, J. A.: Physical and Mechanical Properties of Commercial Molybdenum-Base Alloys. DMIC Rep. 140, Defense Metals Info. Center, Battelle Memorial Inst., Nov. 30, 1960.

5. Meisl, C. J., and Shapiro, A.: Thermodynamic Properties of Alkali Metal Vapors and Mercury. Rep. R60FPD358-A, General Electric Co., Nov. 9, 1960.

6. LaValle, Vincent L., and Huppert, Merle C.: Effects of Several Design Variables on Turbine-Wheel Weight. NACA TN 1814, 1949.

7. Rossbach, R. J.: Implications of Dimerization on Isentropic Processes in Alkali Metals. Rep. DM 61-180, General Electric Co., June 6, 1961.

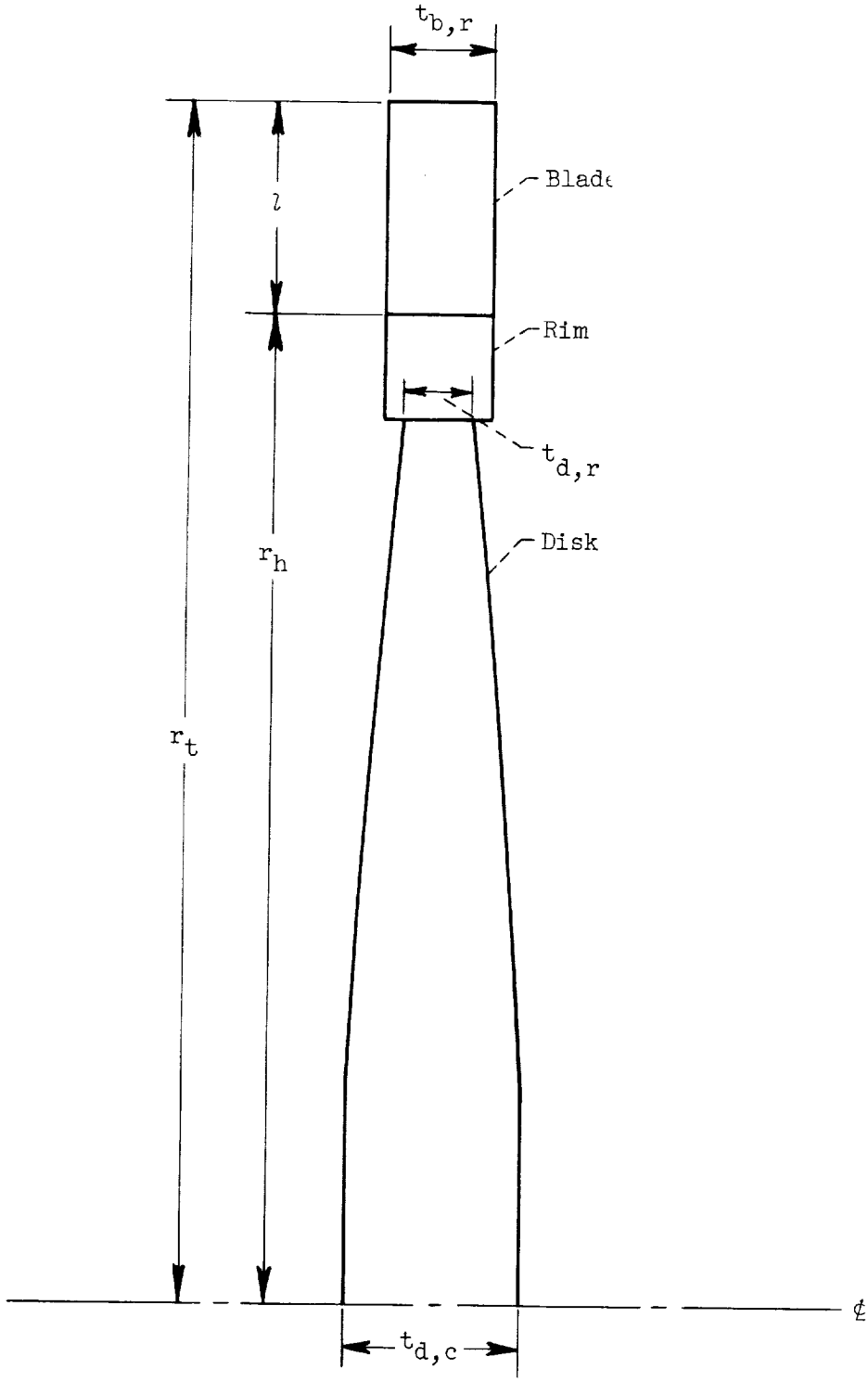


Figure 1. - Typical turbine rotor.

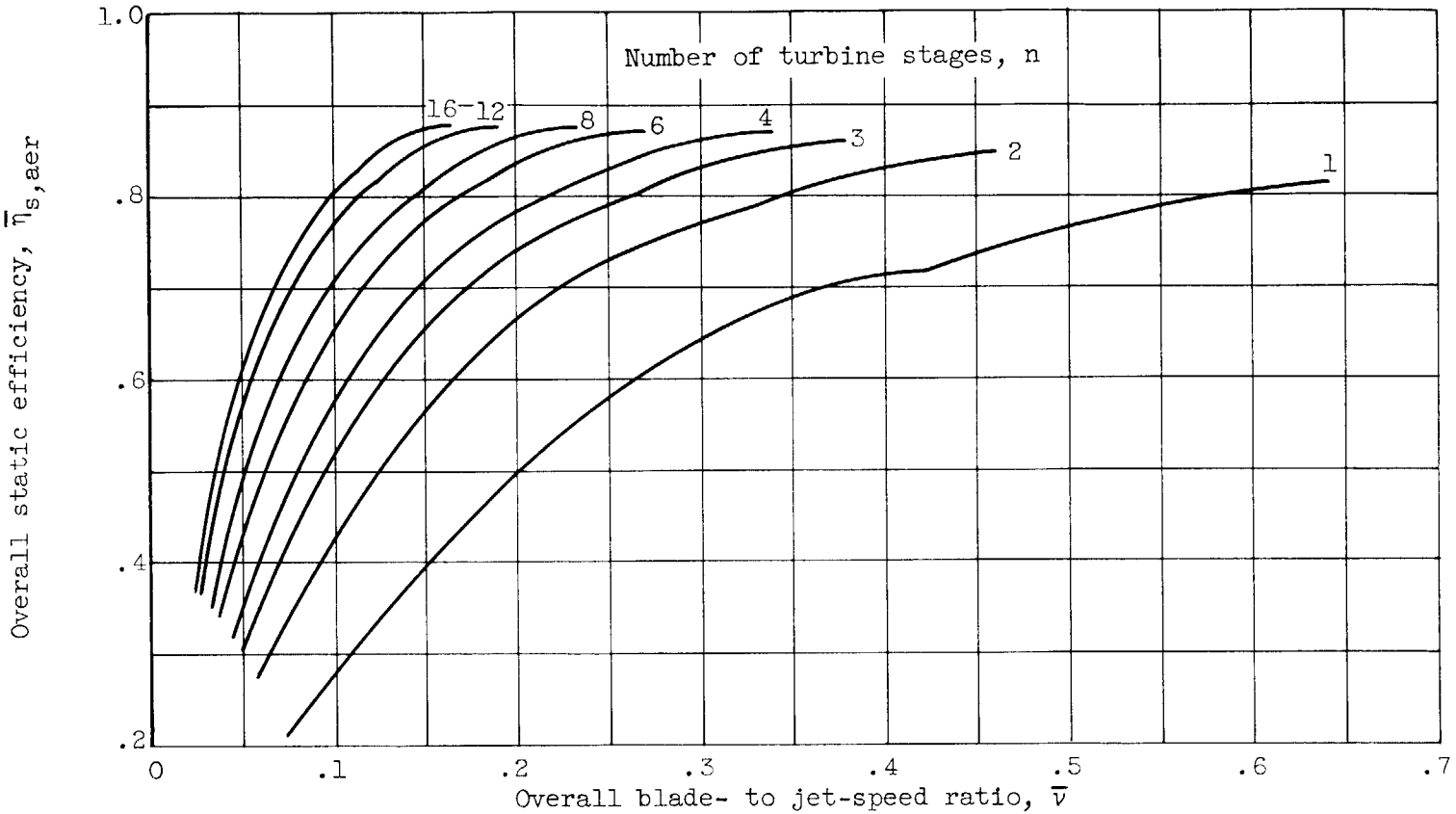


Figure 2. - Multistage turbine static-efficiency characteristics as function of overall blade- to jet-speed ratio. Constant of proportionality K (as defined in ref. 3), 0.4; Reynolds number, $10^6$; mean-section stator-exit angle, 70°; ratio of rotor- to stator-exit kinetic energies, 1.5.

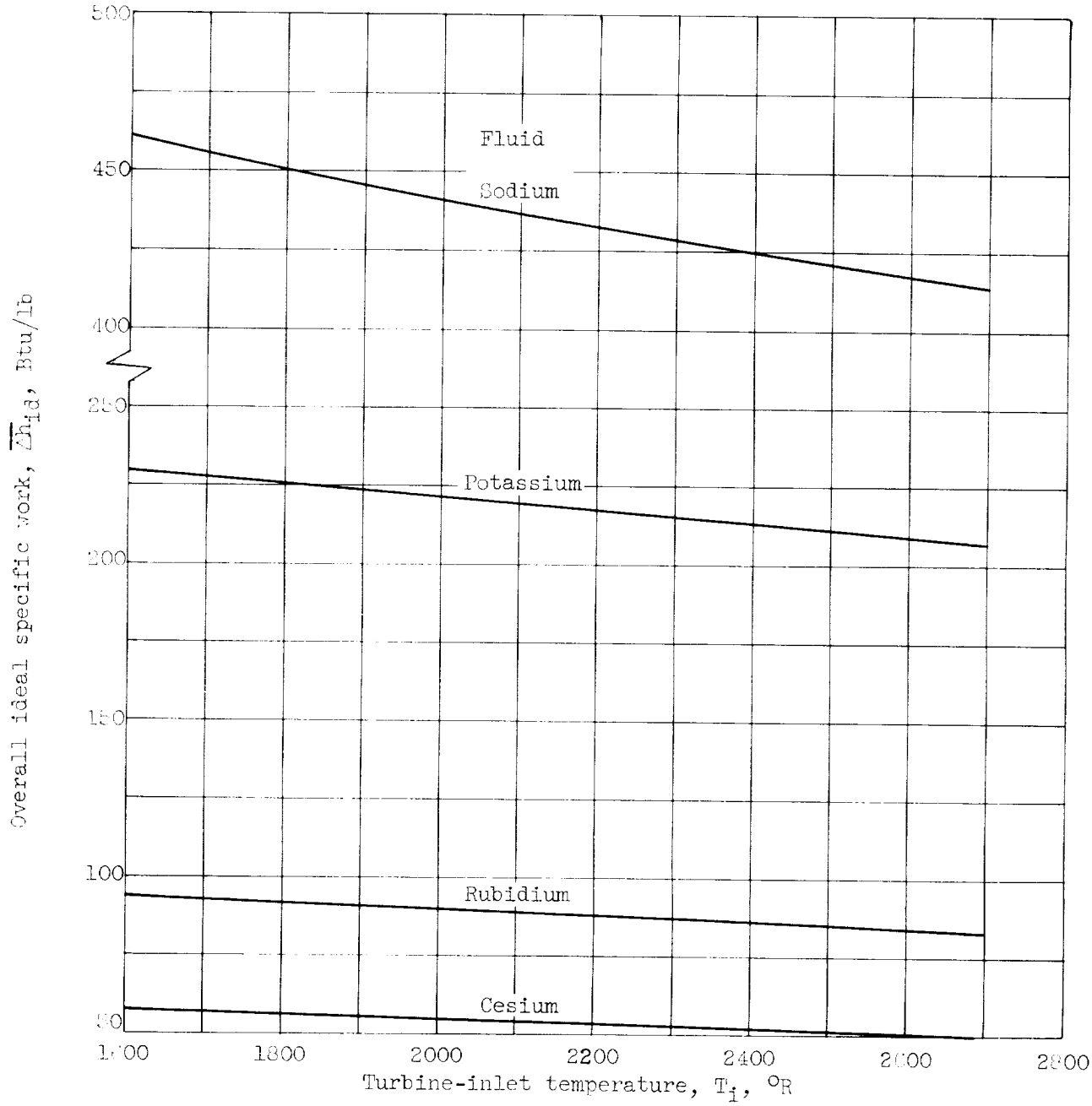


(a) Ideal specific work. Ratio of turbine-exit to -inlet temperature, 0.75.

Figure 3. - Effect of temperature on fluid properties (data obtained from ref. 5).

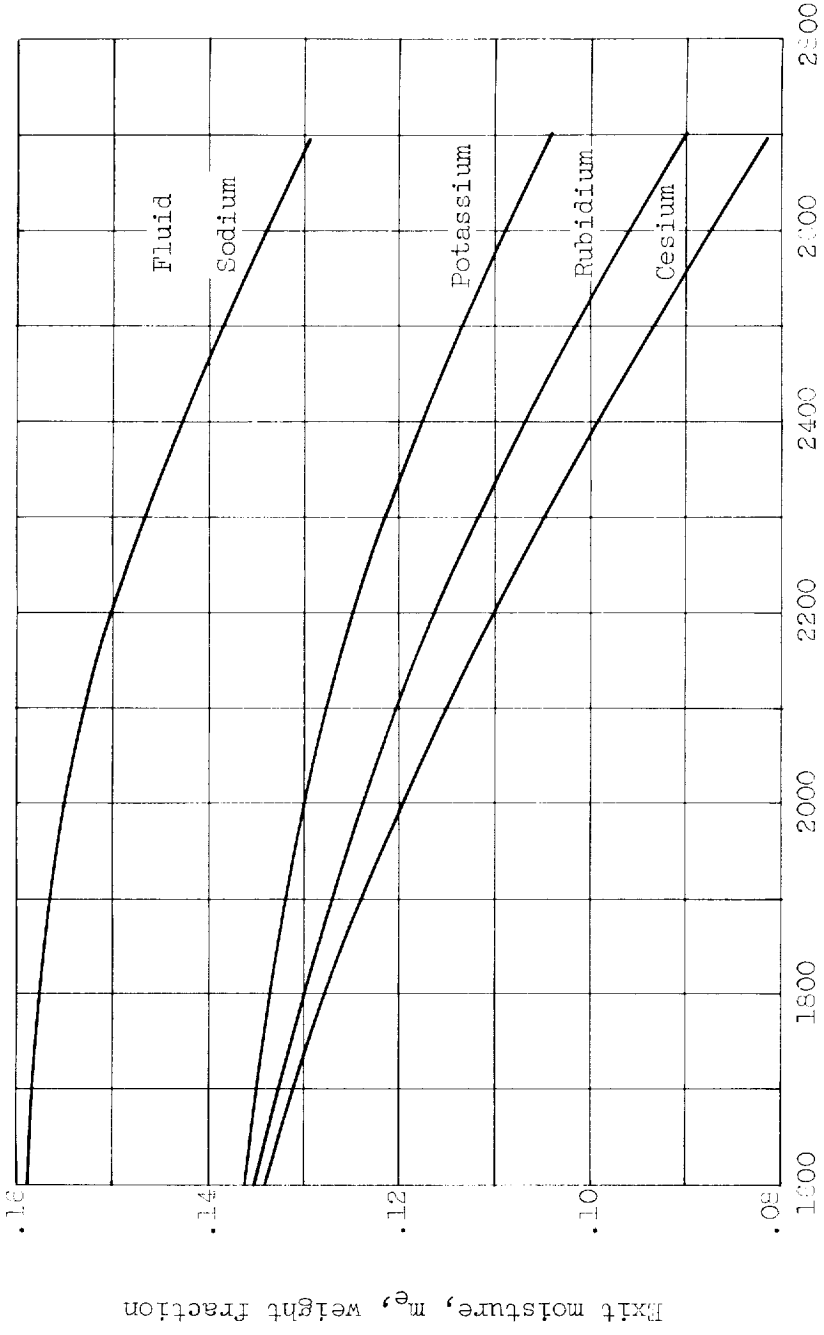


(b) Exit moisture. Ratio of turbine-exit to -inlet temperature, 0.75; overall aerodynamic turbine efficiency, 0.80.

Figure 3. - Continued. Effect of temperature on fluid properties (data obtained from ref. 5).

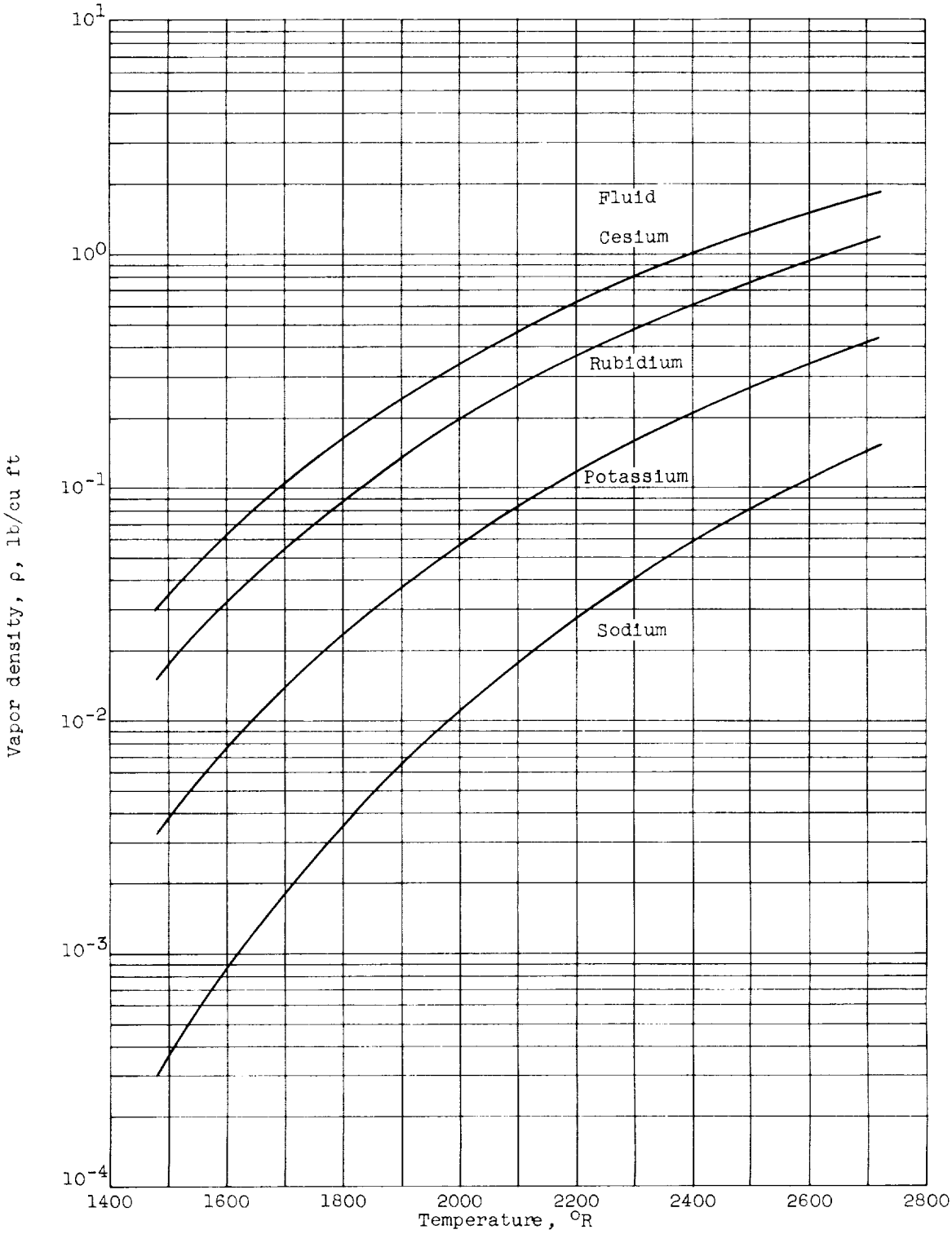


(c) Vapor density.

Figure 3. - Concluded. Effect of temperature on fluid properties (data obtained from ref. 5).

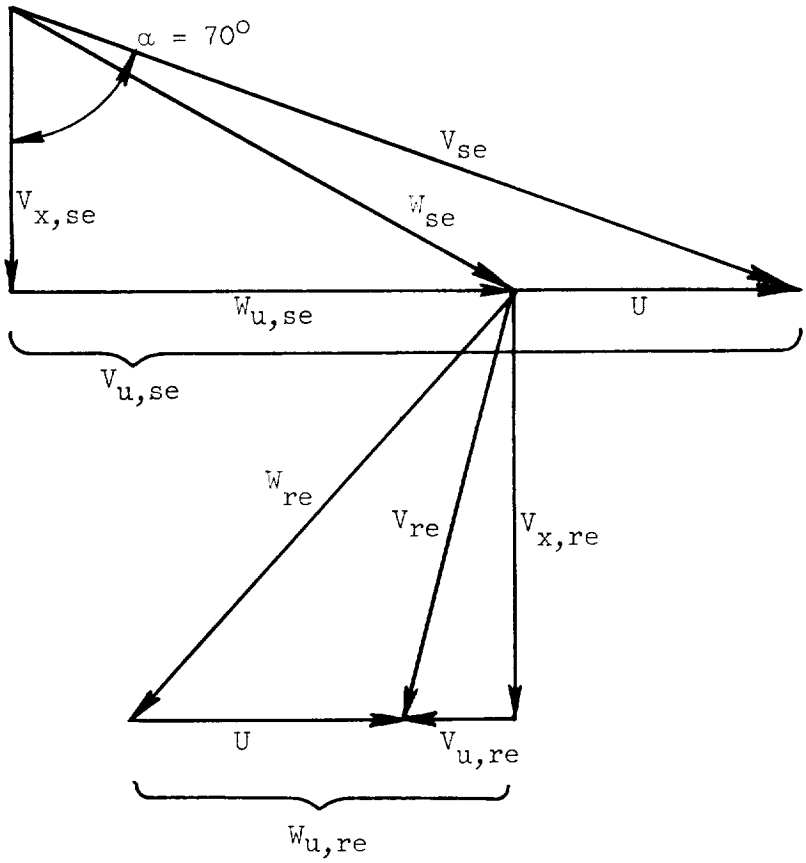


Figure 4. - Typical turbine-stage velocity diagram.

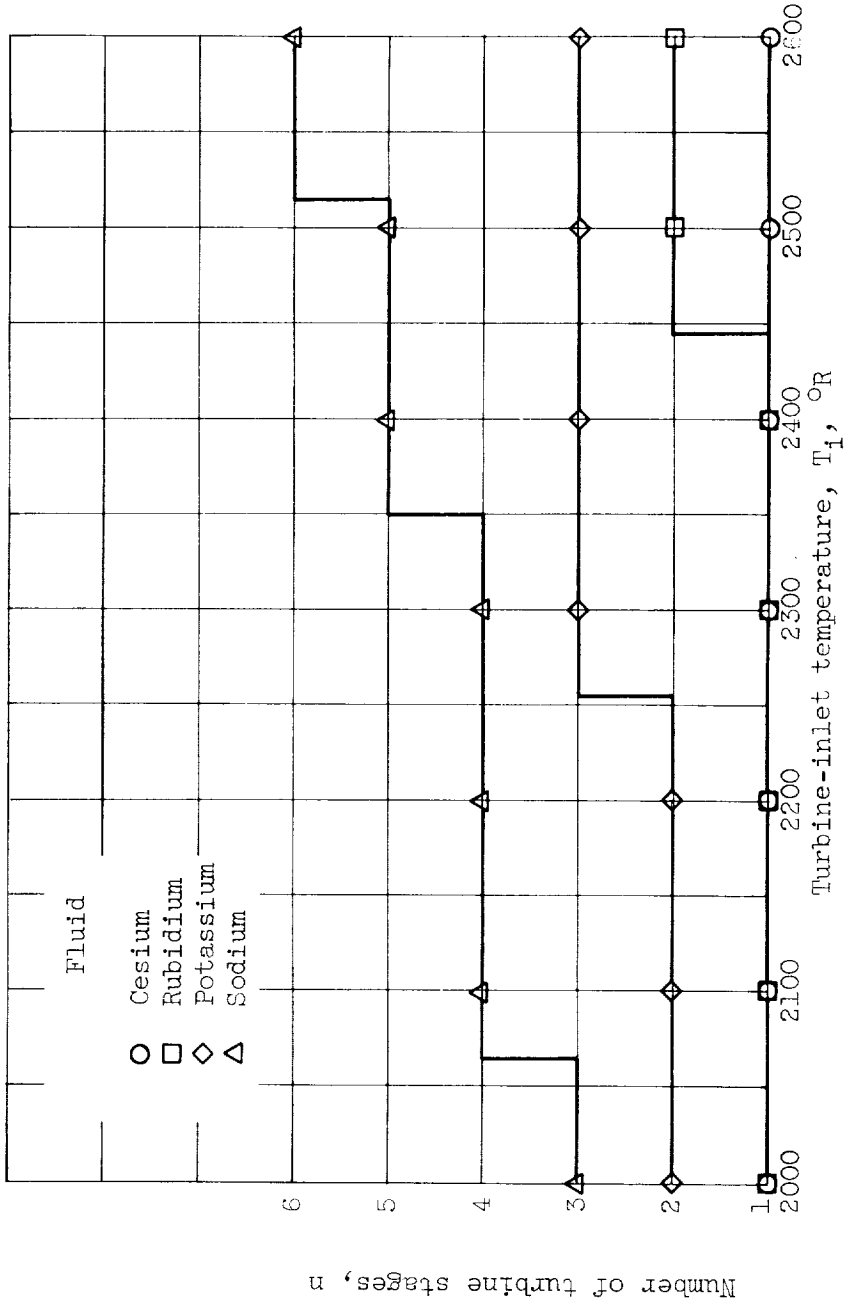


Figure 5. - Required number of turbine stages as function of turbine-inlet temperature.

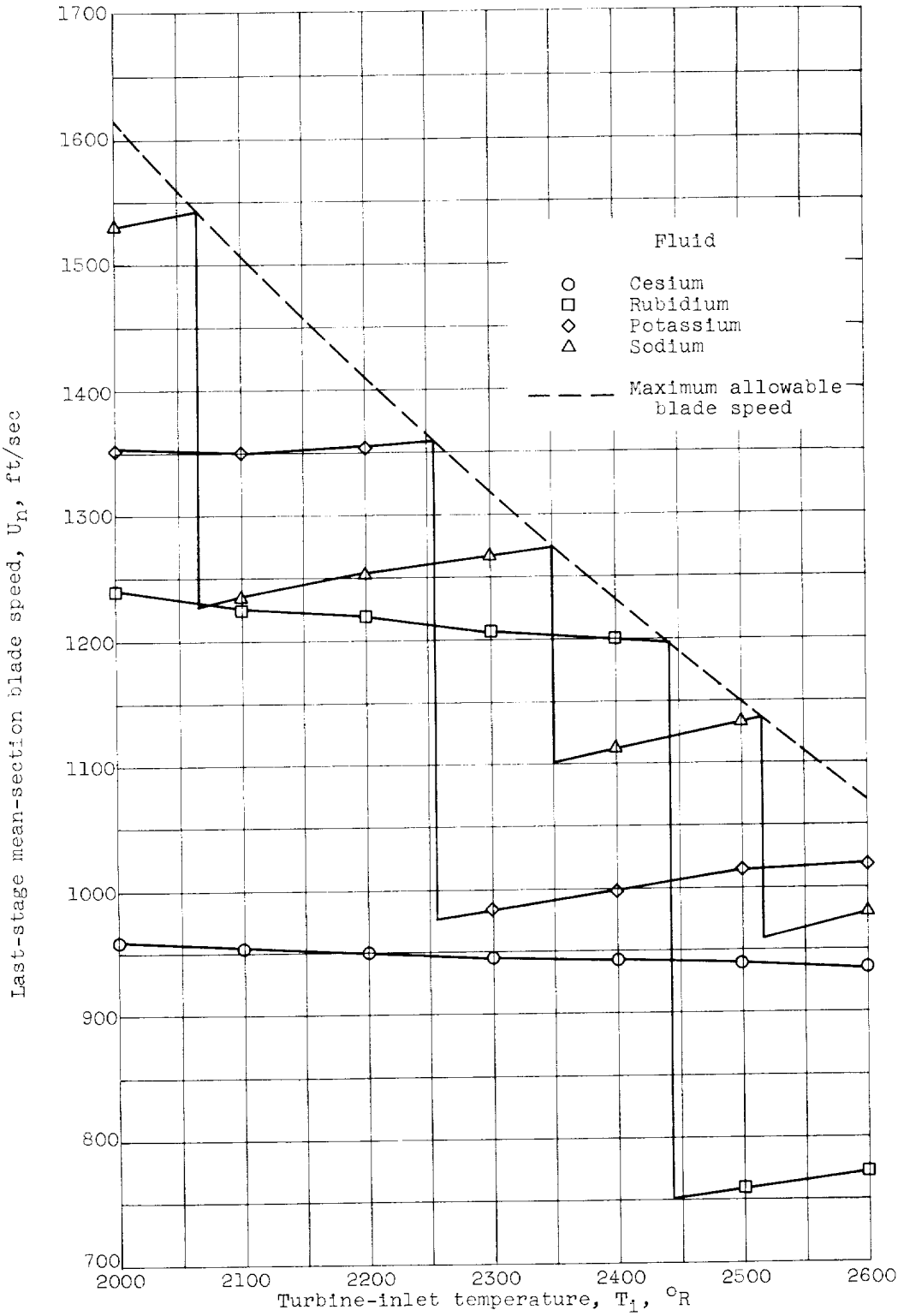


Figure 6. - Last-stage mean-section blade speed as function of turbine-inlet temperature.

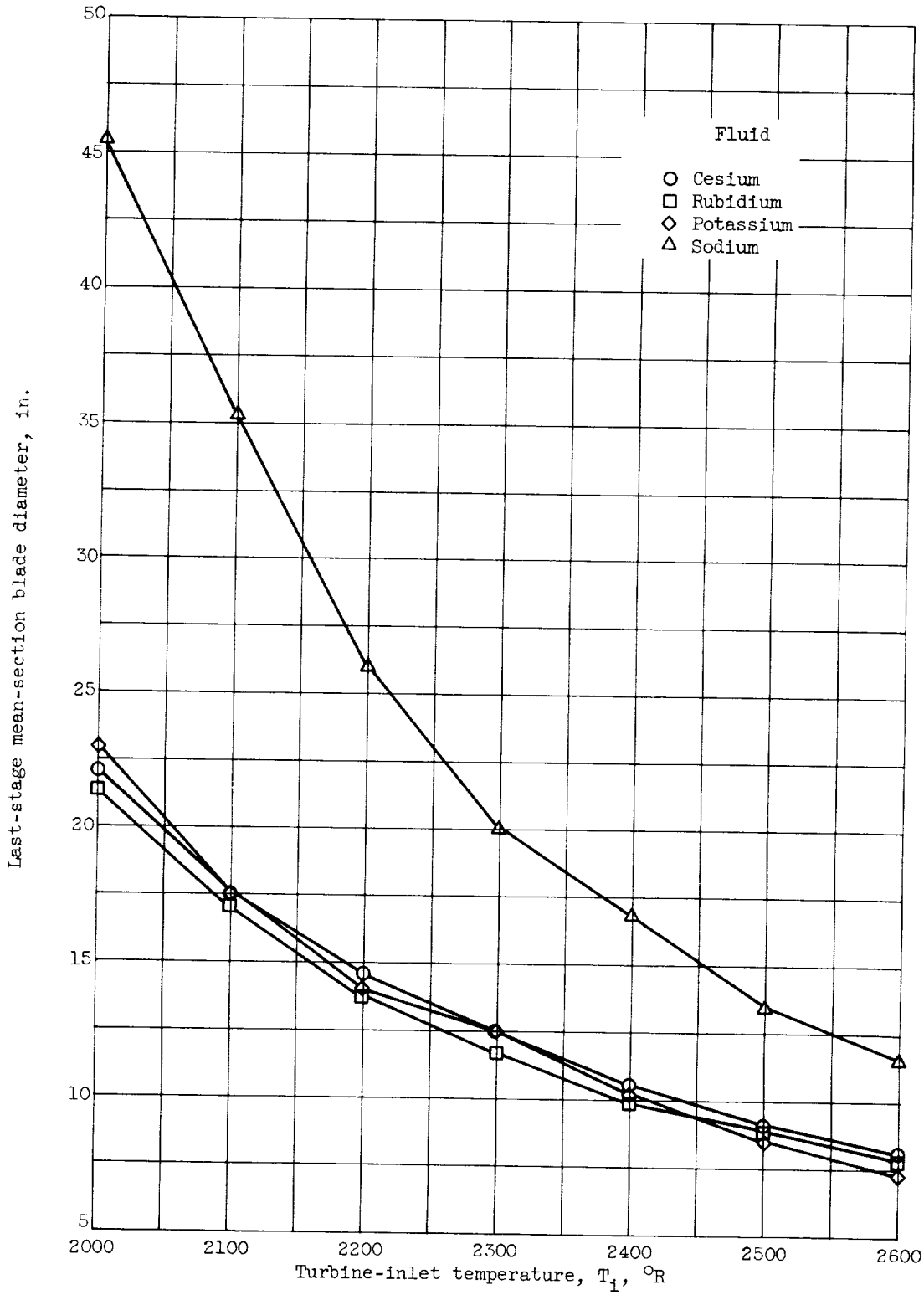


Figure 7. - Last-stage mean-section blade diameter as function of turbine-inlet temperature.

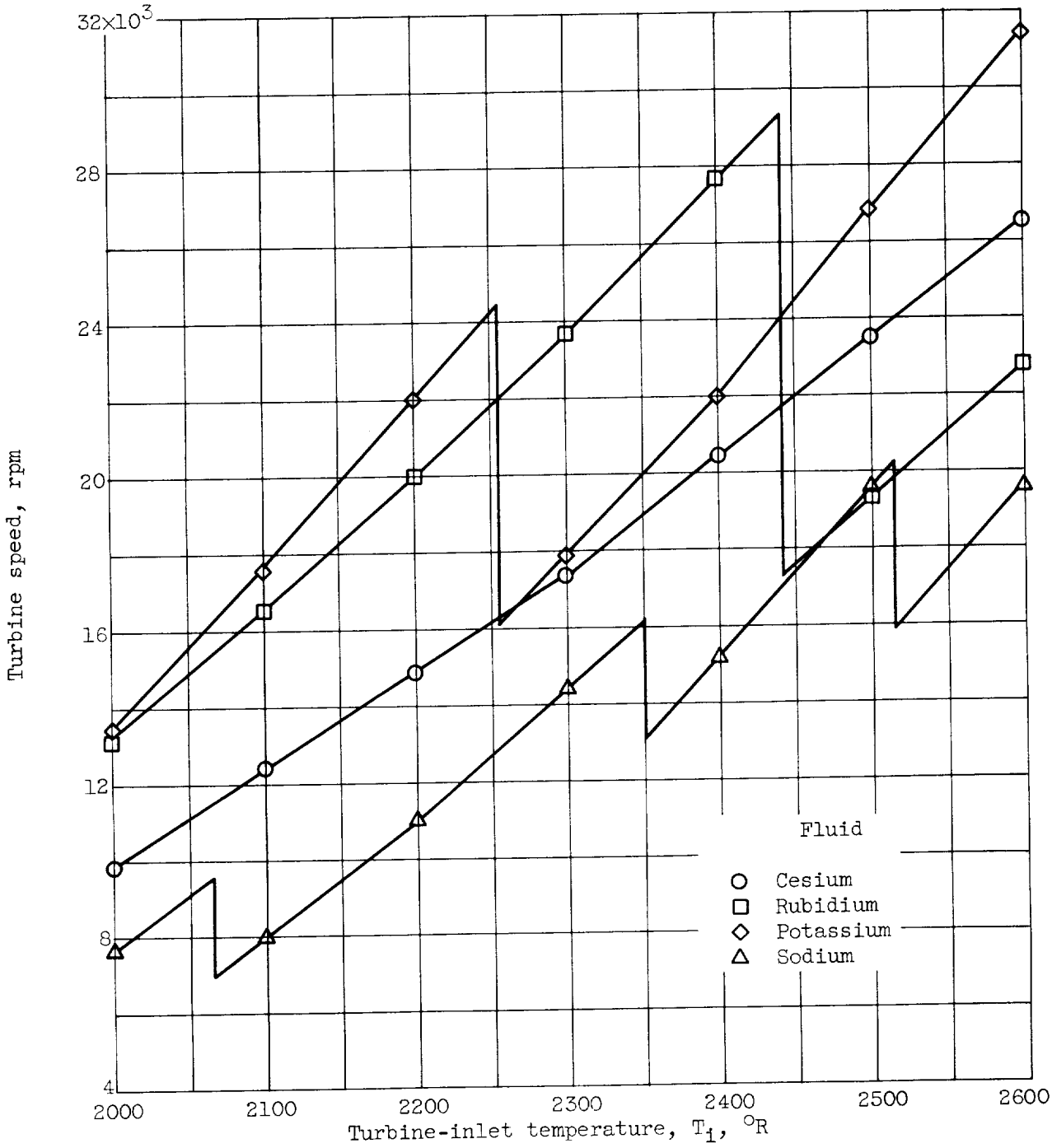


Figure 8. - Turbine rotative speed as function of turbine-inlet temperature.

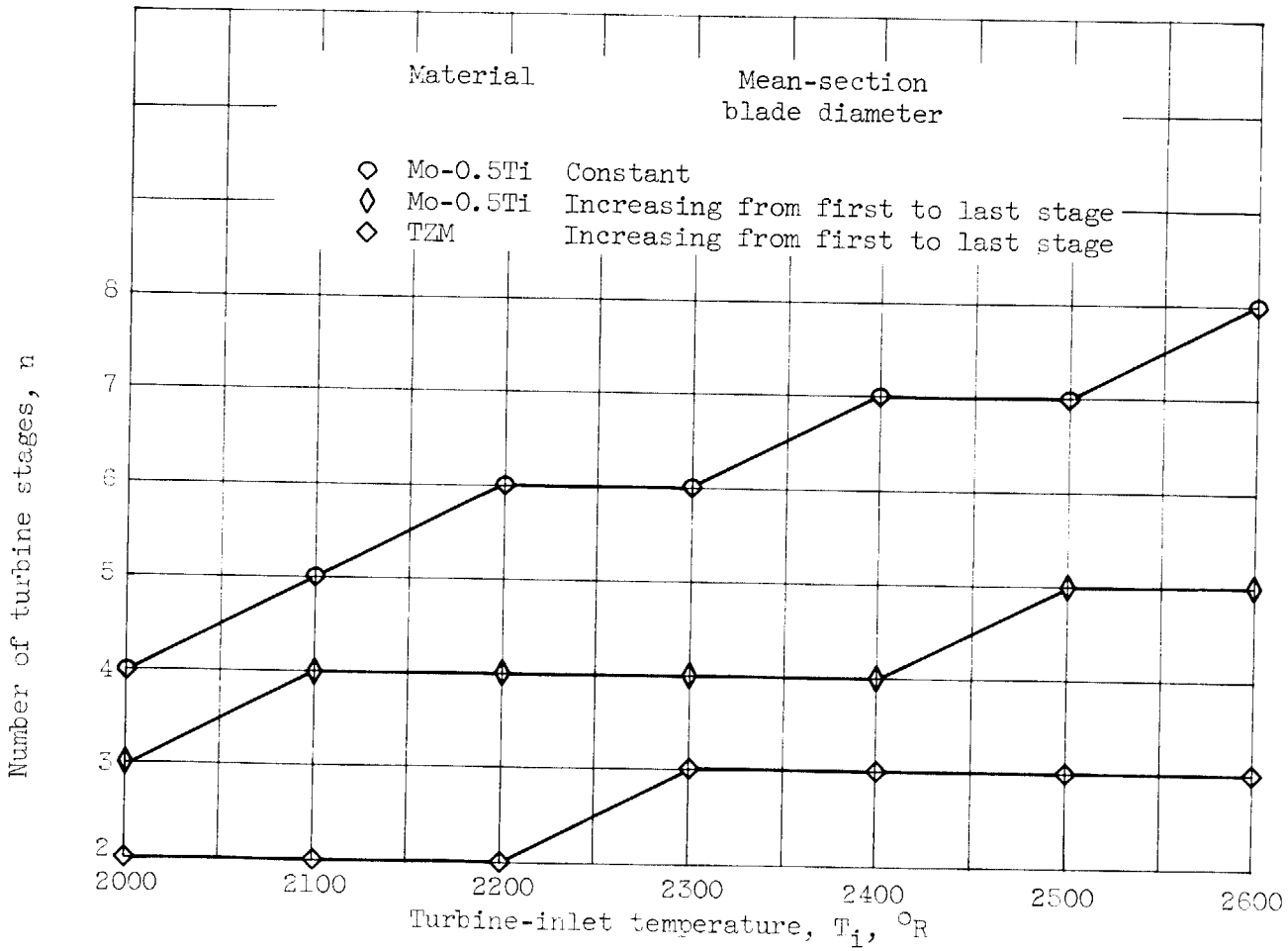


Figure 9. - Number of turbine stages as function of blade-diameter configuration, structural material, and turbine-inlet temperature. Fluid, potassium.

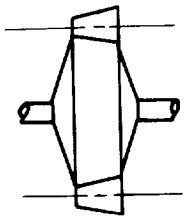

(a) Fluid, cesium; one stage; stage diameter, 9.15 inches; rotative speed, 23,545 rpm.

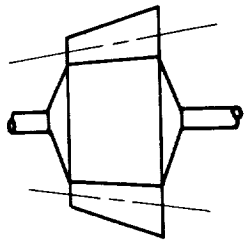

(b) Fluid, rubidium; two stages; diameter of first stage, 7.68 inches; diameter of last stage, 9.00 inches; rotative speed, 19,323 rpm.

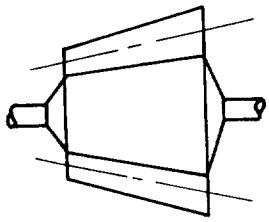

(c) Fluid, potassium; three stages; diameter of first stage, 5.64 inches; diameter of last stage, 8.68 inches; rotative speed, 26,758 rpm.

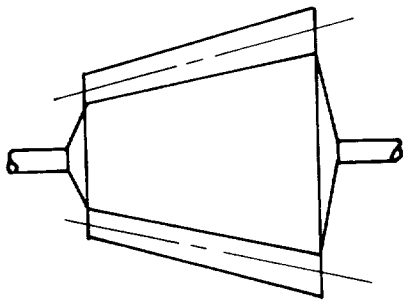

(d) Fluid, sodium; five stages; diameter of first stage, 7.16 inches; diameter of last stage, 13.28 inches; rotative speed, 19,556 rpm.

Figure 10. - Turbine characteristics at turbine-inlet temperature of 2500° R.

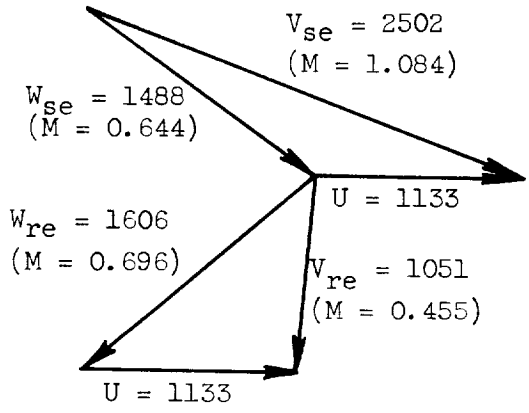


(a) Sodium.

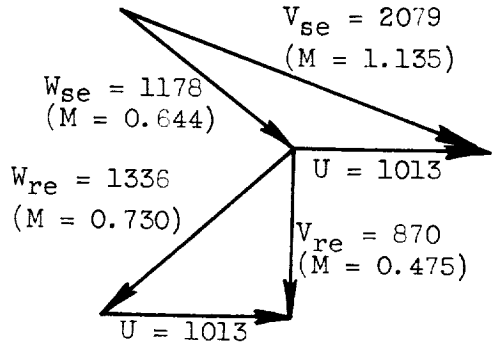


(b) Potassium.

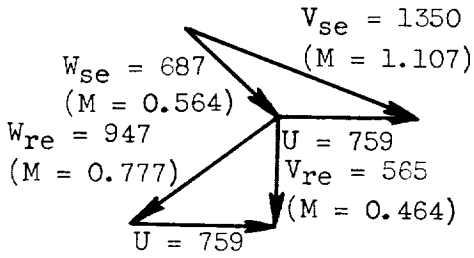


(c) Rubidium.

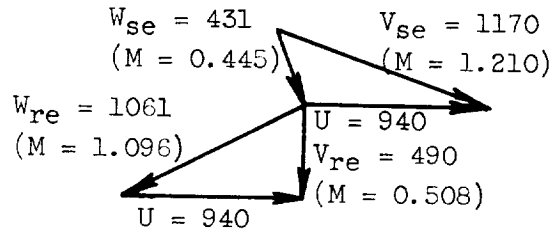


(d) Cesium.

Figure 11. - Last-stage velocity diagrams for turbine-inlet temperature of 2500° R. (Velocities are ft/sec.)